Chapter

4

**Mass Transfer Characteristics
of the
UV-BCR**

*The next best thing to knowing something
is knowing where to find it.
Samuel Johnson (1709-1784)*

4.1 INTRODUCTION

4.1.1 Bubble column reactors

Bubble column reactors (BCR) are multiphase reaction devices in which a discontinuous gas phase moves in form of bubbles relative to the continuous liquid phase. Continuous BCR can be operated concurrently or countercurrently. However, as a result of considerable mixing and the low liquid flow rate usually being applied, counter flow offers no significant advantages. Mass transfer characteristics of BCR depend strongly on the prevailing flow regime. Shah et al. (1982) in their review article give the three different flow regimes as a function of increasing gas flow rate as:

(a) Homogeneous flow regime, characterized by almost uniformly sized bubbles with equal radial distribution, occurring up to superficial gas velocities of approximately 0.05 m/s and bubble rise velocities between 0.18 and 0.3 m/s.

(b) Heterogeneous flow regime, occurring at higher gas velocities where the homogeneous gas-in-liquid dispersion cannot be maintained and an unsteady flow pattern with channeling occurs. The change in the flow regime is characterized by sharp increase in bubble rise velocity.

(c) Slug flow regime, occurring in small diameter bubble columns at high gas flow rates, where large bubbles are stabilized by the column wall leading to the formation of bubble slugs.

The best mass transfer performance is obtained in the homogeneous bubbly flow regime.

Compared with other multiphase reactors (stirred vessels, packed towers, trickle bed reactors, etc.), BCR offer several advantages such as

⚔ Low maintenance due to simple construction and no problems with sealing due to the absence of moving parts;

⚔ High liquid phase content for the reaction to take place;

⤌ Reasonable interphase mass transfer rates at low energy input;

⤌ Excellent heat transfer properties and, hence, easy temperature control;

⤌ Low floor space requirement; and,

⤌ BCR are relatively cheap.

Disadvantages are, however, considerable backmixing in both the continuous liquid phase and dispersed gas phase, high pressure drop (if operated at atmospheric conditions) and bubble coalescence. Since BCR provide high liquid content, and sufficient mass transfer rates, they are well-suited for gas-liquid reactions taking place in the slow reaction-absorption regime.

4.1.2 Mass transfer coefficient

When a soluble gas is transferred by diffusion from a gas phase into a liquid, the molar flux *J* is proportional to the overall concentration driving force and to the overall mass transfer coefficient. Based on the Whitman's "two-film theory" the overall mass transfer coefficients K_G and K_L between the gas and liquid phase are defined as

$$J = K_G(p_G - p_L^*) = K_L(c_G^* - c_L) \tag{4-1}$$

where *J* is the flux of the gas transferred between the phases, K_G is the overall mass transfer coefficient based on the partial pressure driving force, p_G is the partial pressure of the solute in the gas phase, p_L^* is the partial pressure of solute in the equilibrium with its concentration in the bulk liquid phase c_L, K_L is the overall mass transfer coefficient based on the liquid phase concentration driving force, and c_G^* concentration in equilibrium with its partial pressure in the gas phase, p_G. For absorption without chemical reaction the local molar flux at any height may be expressed in terms of individual mass transfer coefficients and the driving force for each phase:

69

$$J = k_G(p_G - p_i) = k_L(c_{L,i} - c_L) \tag{4-2}$$

where k_G is the gas side mass transfer coefficient, k_L is the liquid side mass transfer coefficient, and p_i and c_i are the partial pressure and concentration at the gas-liquid interface, respectively. In dilute aqueous systems at atmospheric pressures and moderate temperatures, most gases obey Henry's law, especially if they are not very soluble. It was in the year of 1803 that William Henry stated that, at constant temperature, the mass of a gas dissolved in a given volume of a solvent is directly proportional to its partial pressure in the gas phase in equilibrium with the solution:

$$p_i = He_i c_{L,i} \tag{4-3}$$

At atmospheric pressures, gas phase approaches ideal behavior:

$$He_i = \frac{y_i p_T}{c_{L,i}} = \frac{n_i}{n_T} \times \frac{n_T R T_e}{V_T c_{L,i}} \tag{4-4}$$

so that a commonly used form of the law can be obtained by rearranging Eq. (4-4):

$$m_i = \frac{He_i}{RT_e} = \frac{c_{G,i}}{c_{L,i}} \tag{4-5}$$

By combination of equations from (4-1) to (4-5), the following expression can be derived:

$$\frac{1}{K_L} = \frac{1}{HeK_G} = \frac{1}{k_L} + \frac{1}{Hek_G} = \frac{1}{k_L} + \frac{1}{mRT_e k_G} \tag{4-6}$$

By multiplying Eq. (4-2) with the interfacial area *a*, the local absorption rate *N* is obtained.

Due to their large liquid content bubble columns are primarily meant for the gas-liquid absorption processes accompanied by a slow reaction. In this case, the volumetric mass transfer coefficient, $k_L a$, defines the mass transfer between the flowing phases reasonably well. Thus, there is no need to split this parameter into the liquid side mass transfer coefficient, k_L, and the specific interfacial area, a. However, this is not the case for fast and instantaneous reactions.

Determination of mass transfer parameters in bubble column reactors has been a subject of numerous studies and publications (Deckwer and Shumpe, 1993; Munz and Roberts, 1989; Roberts *et al.*, 1984; Shah *et al.*, 1982). It was shown that the *a priori* design of bubble columns is still difficult, due to the fact that the bubble properties (bubble size and shape, bubble velocity and interfacial area) in gas liquid dispersions depend largely on reactor geometry, operating conditions, gas distribution and physico-chemical properties of the two phases. Bubble behavior has a direct bearing on hydrodynamics, mass transfer and reactor performance. Therefore, it is always useful if the mass transfer characteristics of a given reactor are determined experimentally. Sometimes, due to the lack of ability for experimental capability literature correlations may be used as an order of magnitude approximation. Among the correlations found in the opened literature, Deckwer and Shumpe (1993) recommend the following three in particular, as they have been proven to be of broader applicability.

Akita and Yoshida (1973) performed the experimentation of various gas-liquid systems assuming total dispersion of the liquid phase and plug flow of the gas phase, and proposed the following dimensionless correlation

$$\frac{k_L a \cdot d_R^2}{D_L} = 0.6 \left(\frac{\eta_L}{\rho_L D_L} \right)^{0.5} \left(\frac{g d_R^2 \rho_L}{\sigma} \right)^{0.62} \left(\frac{g d_R^3 \rho_L^2}{\eta_L^2} \right)^{0.31} \varepsilon_G^{1.1} \tag{4-7a}$$

or

$$Sh = 0.6Sc^{0.5}Bo^{0.62}Ga^{0.31}\varepsilon_G^{1.1} \qquad (4\text{-}7b)$$

By considering the correlation of Akita and Yoshida for ε_G, which was found to be proportional to the superficial gas velocity on power 0.64, and neglecting the dependency of physical properties, equation (4-7) reduces to

$$K_La \propto d_R^{0.17}u_G^{0.7} \qquad (4\text{-}8)$$

Equation (4-8) is consistent with the experimental observations of other authors, indicating that the gas superficial velocity has a major impact on the volumetric mass transfer coefficient. Even the well-known Kastanek's expression for k_La evaluation

$$k_La = \frac{u_G(u_G + C)^{13/20}}{2u_G + C} \qquad (4\text{-}9)$$

which was derived on the basis of the Higbie mass transfer theory and the Kolmogoroff theory of isotropic turbulence, can be reduced to a simple form

$$k_La = bu_G^n. \qquad (4\text{-}10)$$

Both parameters are empirical constants. The liquid phase properties and the type of the distributor strongly affect the value of *b*, whereas the exponent *n* is rather insensitive to both of them over a wide range of superficial gas velocities. Deckwer *et al.* (1974) confirmed the above assumptions and found out *n* to be in the range of 0.78-0.82, and *b* to be affected by both, gas distributor and the liquid properties. In contrast to the observations of Akita and Yoshida, in their analysis of measured O_2 concentration profiles Deckwer *et al.* applied the axial dispersion model (ADM) for the liquid phase.

Hikita *et al.* (1981) proposed another correlation, which also incorporates the gas viscosity as

$$\frac{k_L a \cdot u_G}{g} = 14.9 \cdot f \left(\frac{u_G \eta_L}{\sigma}\right)^{1.76} \left(\frac{\eta_L^4 g}{\rho_L \sigma^3}\right)^{-0.248} \left(\frac{\eta_G}{\eta_L}\right)^{0.243} \left(\frac{\eta_L}{\rho_L D_L}\right)^{-0.604} \tag{4-11}$$

in which f = 1 for non-electrolytes (water, methanol, butanol, etc) and is a function of ionic strength in case of electrolyte solutions.

Comprehensive $k_L a$ data were obtained for organic liquids and different gases (CO_2, Air, N_2, O_2, H_2) by Öztürk *et al.* (1987). In their study, they performed more than 400 measurements in different gas liquid systems. However, correlations of Hikita *et al.* (Eq. (4-11)) and Akita and Yoshida (Eq. (4-7)) described the experimental data with errors of 25 to 37%. They Therefore proposed a new correlation using the Akita-Yoshida correlation as a basis. Since column diameter has a low influence on mass transfer coefficient, they have changed the characteristic length from the reactor diameter to the surface-to-volume mean bubble diameter, d_B, which has a more important role. The d_B was assumed to be approximately constant (d_B = 0.003 m) as recommended by several authors. The correlation obtained by a non-linear regression analysis is as follows:

$$\frac{k_L a \cdot d_B^2}{D_L} = 0.62 \left(\frac{\eta_L}{\rho_L D_L}\right)^{0.5} \left(\frac{g d_B^2 \rho_L}{\sigma}\right)^{0.33} \left(\frac{g d_B^3 \rho_L^2}{\eta_L^2}\right)^{0.29} \left(\frac{u_G}{\sqrt{g d_B}}\right)^{0.68} \left(\frac{\rho_G}{\rho_L}\right)^{0.04} \tag{4-12}$$

and involves the following dependencies:

$$k_L a \propto D_L^{0.5} \rho_L^{0.37} \eta_L^{0.08} \sigma^{-0.33} \rho_G^{0.04} u_G^{0.68} \tag{4-13}$$

Even though the above mentioned empirical correlations have been recognized as an important tool in predicting mass transfer coefficients, it is always useful if the mass transfer

characteristics of a given reactor are determined experimentally. As the annular reactor configuration is not so commonly used in gas absorption processes, I felt a need to determine and confirm the mass transfer coefficient experimentally.

Mass transfer measurements can be performed by either chemical or physical methods under dynamic or steady state conditions, each of them having their advantages and limitations (Charpentier, 1981; Gaddis, 1999).

For measurement of oxygen absorption in water, a chemical method such as sulfite method may be used. Aqueous sodium sulphite is oxidized in the presence of catalyst into sodium sulphate by means of molecular oxygen dissolved in water. From the knowledge of the kinetics of the chemical reaction and the depletion of sodium sulphite in the solution with time, the $K_L a$ value can be calculated. One of the main disadvantages of the sulphite method is the relatively high residual salt concentration in the water, which influences the coalescence of bubbles. The bubble diameter decreases as a result of the presence of the salt and the total interfacial area of gas bubbles present in the liquid for a given gas hold-up increases; the corresponding $K_L a$ value may increase largely. This method is thus not suitable for a coalescent system.

If the dynamic physical method is used, the oxygen is first desorbed from the liquid by bubbling an inert gas (e.g. nitrogen) through the liquid until the concentration of dissolved oxygen in the contactor drops to a low level. Nitrogen flow is then stopped and oxygen or air is fed in the contactor. The change of the oxygen concentration in the liquid with time is measured with an electrode and recorded by a suitable device. The $K_L a$ value is then calculated from a model equation describing the hydrodynamic behavior of the bubble column (e.g. ideal mixing, plug flow, or axial dispersion model). The adequacy of this method depends on the ratio of the time constant of the contractor to the time constant of the electrode.

Due to chemical handling and analytical difficulties, measurement of the CVOC mass transfer coefficient is significantly more challenging than measuring the oxygen $K_L a$. Therefore, the ability to estimate $K_L a$ values for any CVOC from $K_L a(O_2)$ values is desired. Several authors (Matter-Muller *et al*., 1981; Roberts and Dandliker, 1983; Hsieh *et al*., 1993; Bielefeldt and Stensel, 1999) reported the applicability of the relation

$$\frac{k_L a_{CVOC}}{k_L a_{O_2}} = \left(\frac{D_{CVOC}}{D_{O_2}} \right)^n \cong \frac{K_L a_{CVOC}}{K_L a_{O_2}} \tag{4-14}$$

for prediction of mass transfer coefficient with different successes. The relation holds only for the processes where the liquid film resistance controls the mass transfer of both CVOC and the oxygen. The exponent in Eq. (4-14) was reported in the range between 0.5 and 1, based on penetration and film theories and their predictions of the dependencies of mass transfer coefficient on the diffusivity. Success of the application of Eq. (4-14) was reported differently, from a very good agreement (surface aeration with n = 0.66, Roberts and Dandliker, 1983), to no agreement at all (diffused aeration stripping of CVOCs and oxygen, Hsieh *et al.,* 1993).

With such a diverse reports on prediction possibilities, a model for estimation of the volumetric mass transfer coefficient for PCE and other volatile organic compounds is presented in the following section and later compared with other models.

4.2 MODEL DEVELOPMENT

The fundamental differential equation that describes the change in the PCE concentration in the bubbles of contaminated gas sparged into the reactor as they rise through the liquid can be written as:

$$-u_G \frac{dc_P^G(z,t)}{dz} - \alpha \cdot K_L a \left(\frac{c_P^G(z,t)}{m} - c_P^L(t) \right) = 0 \qquad (4\text{-}15)$$

with boundary conditions set as $z = 0$; $c_P^G(0, t) = c_P^{G,IN}$ and $z=h$; $c_P^G(h, t) = c_P^{G,OUT}$.

With the assumptions that the overall mass transfer coefficient K_L is constant over the depth; that the equilibrium at the bubble-liquid interface obeys Henry's law; and that the air flow rate and temperature are constant and although the PCE concentration in the rising bubbles are changing with depth in the reactor, the liquid concentration in the reactor can be considered to be constant in a well mixed reacting system at steady-state. Under steady-state conditions, Eq. (4-15) can be solved for the concentration in the effluent gas, yielding Eq.(4-16).

$$c_G^{out} = c_G^{in} \cdot \exp\left(-\frac{\alpha \cdot K_L a \cdot h}{m \cdot u_G} \right) + m \cdot c_L \left[1 - \exp\left(-\frac{\alpha \cdot K_L a \cdot h}{m \cdot u_G} \right) \right] \qquad (4\text{-}16)$$

For calculations of $K_L a$ assuming that there is no PCE in the inlet gas Eq. (4-16) can be combined with Eq.(4-17)

$$-\frac{dc_{PCE}^L}{dt} = \frac{u_G}{h} c_{PCE}^{G,OUT} \qquad (4\text{-}17)$$

which can then be integrated and expressed as Eq.(4-18)

$$\ln \frac{c_{PCE}^{L}(t)}{c_{PCE}^{L}(0)} = -\frac{u_G \cdot m \cdot t}{h}\left[1 - \exp\left(-\frac{K_L a \cdot h}{m \cdot u_G}\right)\right] \qquad (4\text{-}18)$$

Volumetric mass transfer coefficients were calculated from the slopes of $\ln(c_t/c_0)$ vs time plots for different gas superficial velocities, with the dimensionless Henry's constant m calculated for the operating temperature using the relationship of Munz and Roberts (1989), as

$$K_L a = -\frac{u_G \cdot m}{h} \ln\left(1 - \frac{slope \cdot h}{m \cdot u_G}\right) \qquad (4\text{-}19)$$

The evaluation of $K_L a$ in this way is straightforward, using easily measurable parameters.

4.3 EXPERIMENTAL

$K_L a$ was measured in a set of stripping experiments in the UV-BCR. For this purpose the reactor was filled with distilled water, after which a specific volume of PCE saturated solution was added into the reactor to give the desired concentrations of PCE in the liquid. In the beginning target was set to low initial concentrations around 1 mg/L. As the effects of increased PCE concentration seemed to increase mass transfer, higher initial concentrations of cca 10 mg/L were also tested in later runs. Special care was taken to prevent any leakage and to ensure that the solutions were well mixed before the start of the experiment. In those runs, the PCE gas source was disconnected from the reactor system and UV light was turned off. Initial liquid samples were taken in the moments before and after the introduction of air into the system. Those concentrations were compared and used as the concentration at time zero. Liquid samples were taken at regular intervals (from 2 minutes at the beginning to 5

77

minutes after sixth sample) and analyzed for PCE content by GC-ECD.

Gas hold-up was determined by measuring the liquid tower height in the UV-BCR with and without bubbling and was calculated according to

$$\varepsilon_G = \frac{h_b - h}{h_b} \qquad (4\text{-}20)$$

Mass transfer experiments were performed with different gas flow rates ranging from 0.5 to 3.0 L/min. In some runs the sequence-making internal component designed to separate the reactor space into 6 compartments was inserted into UV-BCR to evaluate the influence of gas hold-up on the reactor performance. Flow rates were selected such that bubbles rising through the liquid would not reach the saturation value and thereby suppress the mass transfer (Roberts, Munz and Dändliker, 1984).

4.4 RESULTS AND DISCUSSION

The most important parameter characterizing hydrodynamic behavior of a bubble column reactor is the volume averaged gas hold-up. Knowledge of its value is essential for design and scale-up purposes. Figure 4.1 summarizes the ε_G versus u_G data obtained in two configurations of UV-BCR: with and without the sequence making internal component. These typical results, which agree with literature data (Deckwer and Schumpe, 1993, Shah *et al.*, 1982), demonstrate the significant influence of gas distribution and the presence of the internal component on hydrodynamics. When the internal component was not in the reactor, the gas hold-up was linearly proportional to the gas superficial velocity, indicating the homogeneous bubbly flow regime. However, when internal was in the reactor, the shape of the dependency was typical of a churn-turbulent or transition flow regime.
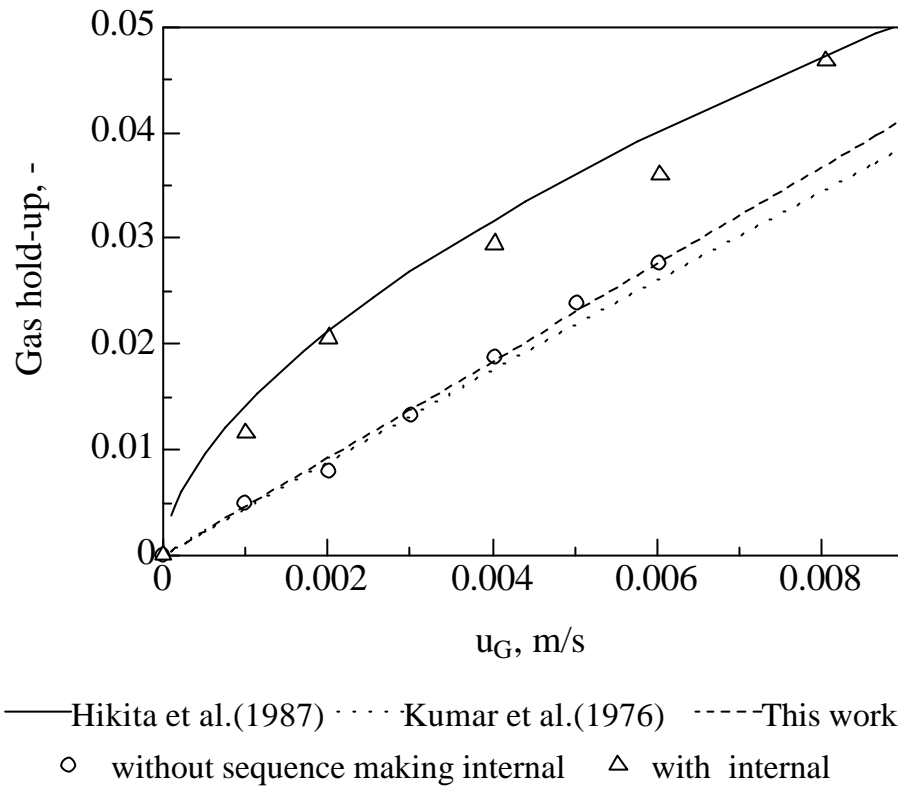
Figure 4.1. Gas hold-ups as a function of gas superficial velocity for UV-BCR with and without the sequence making internal component.

This regime is not likely to occur under such a low superficial gas velocities. However, the presence of the internal component in the UV-BCR could have caused an increase in coalescence of bubbles under its blades and therefore contributed to the additional creation of larger bubbles with non-uniform size and gas composition. For more detailed analysis of the flow regime, the classical drift-flux theory can be applied (Shah *et al.*, 1982; Camarasa *et al.*, 1999). In batch operation, for the liquid, the slip velocity (or the relative velocity between the phases) is defined as:

$$u_S = \frac{u_G}{\varepsilon_G} \pm \frac{u_L}{\varepsilon_L} \qquad (4\text{-}21)$$

and the drift flux as :

$$j_{GL} = u_S \varepsilon_G (1 - \varepsilon_G) = u_G \varepsilon_L \pm u_L \varepsilon_G \qquad (4\text{-}22)$$
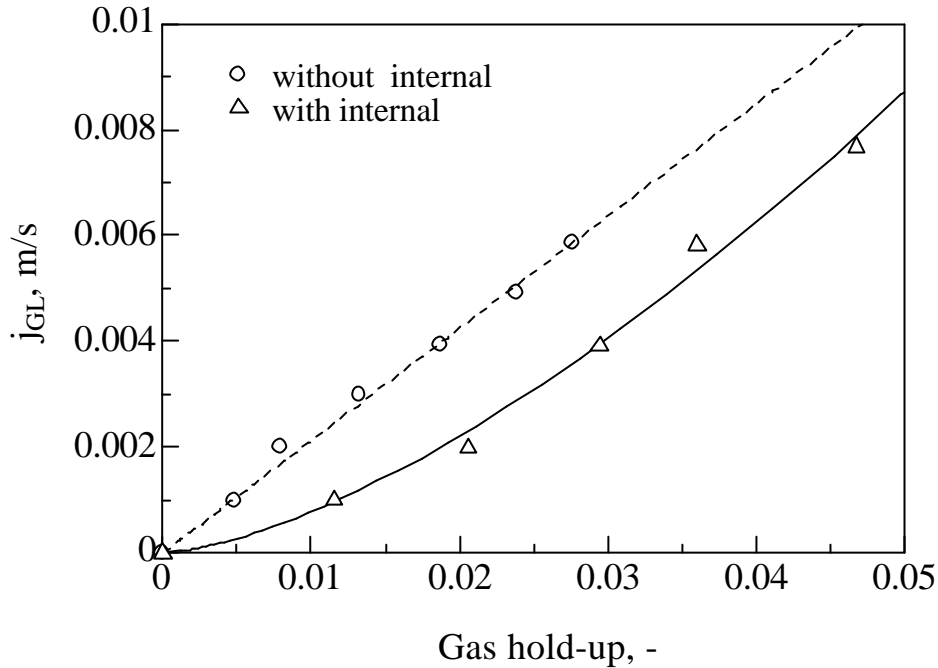

Figure 4.2. Characterization of flow regime with drift-flux analysis.

The plot of j_{GL} versus ε_G immediately reveals which regime prevails in the column as can be observed in Fig. 4.2. The homogeneous regime is characterized by a linear dependency of j_{GL} with gas hold-up up to the point where transition occurs. However, this does not happen under the low superficial gas velocities applied in this study for the experiments not using the internal component. The bubble rise velocity is constant at 21.2 cm/s. On the other hand, with the sequence-making internal component in the reactor, hindrance of the bubble rise by the internal component and the exponential dependency on gas hold-up is observed, as is typical for the transition regime. Since gas hold-up was also linearly proportional to the superficial gas velocity and could be related to the expression $\varepsilon_G = 4.595 u_G$, and since low gas superficial velocities were applied, the reactor was assumed to have been operating in the homogenous

flow regime when internal component was not in the UV-BCR. The correlation of Kumar *et al.* (1976)

$$\varepsilon_G = 0.728U - 0.485U^2 + 0.0975U^3 \tag{4-23}$$

with

$$U = u_G \left(\frac{\rho_L^2}{\sigma(\rho_L - \rho_G g)} \right)^{0.25} \tag{4-24}$$

was derived under similar operational conditions (u_G from $0.0014 - 0.14$ m/s, and d_R between 0.05 and 0.1m) and is in good agreement with our observations for the homogeneous flow regime. However, correlation proposed by Hikita *et al.* (1980)

$$\varepsilon_G = 0.672 \cdot f \left(\frac{u_G \eta_L}{\sigma} \right)^{0.578} \left(\frac{\eta_L^4 g}{\rho_L \sigma^3} \right)^{-0.131} \left(\frac{\eta_G}{\eta_L} \right)^{0.107} \left(\frac{\rho_G}{\rho_L} \right)^{-0.062} \tag{4-25}$$

with f = 1, for non-electrolytes covers the data obtained in a UV-BCR with sequence-making internal component very well. Correlation of Hikita was obtained under heterogeneous flow conditions with u_G ranging from 0.042 to 0.38 m/s. Observations of this study are in agreement with the report of Shah *et al.* (1982) which gives the dependency of gas hold-up as a function of superficial gas velocity raised to an exponent *n*, values of which depend on the flow regime. In the homogeneous bubbly flow regime, the n value varies from 0.7 to 1.2 and in the transition regime, the dependency is less pronounced and varies between 0.4 and 0.7.
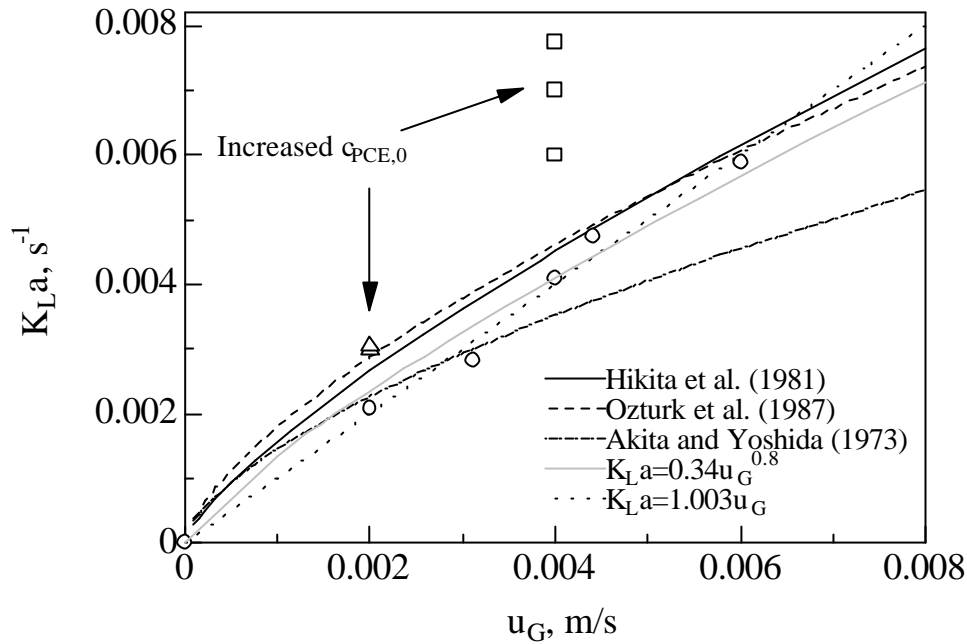
Figure 4.3. $K_L a$ as a function of the superficial gas velocity.

Figure 4.3 shows the influence of the superficial gas velocity on the $K_L a$ coefficient in a UV-BCR together with the predictions obtained by correlations from the literature. The volumetric mass transfer coefficient was linearly proportional to the superficial gas velocity, $K_L a = 1.003 u_G$, (r=0.989) in the low range of superficial velocities tested. However, data could also be fitted to the relation proposed by Deckwer *et al*. (1974), i.e. $K_L a = b u_G^{0.8}$, with b value of 0.34 for this particular sparger (r=0.976). Predicted values represented by circles were obtained in stripping experiments where the initial PCE concentration was set as cca 1 mg/L. When the effect of the initial concentration on the mass transfer coefficient was tested, an interesting phenomena was observed, in which the volumetric mass transfer coefficient increased with increasing initial PCE bulk concentration, which is somewhat unusual. It can be however explained by the possible change in the surface tension of the water due to the presence of the hydrophobic phase (PCE) as reported by Gurol and Nokouinaini (1985) and Camarasa *et al*. (1999). They have shown that the small amounts of chlorinated phenols in the first case and alcohols in second case caused a decrease in the coalescence rate and therefore

increased the mass transfer performance while operating with diffuser-type spargers. Using a single orifice sparger did not affect mass transfer rates, indicating the importance of the gas sparger on the reactor design.
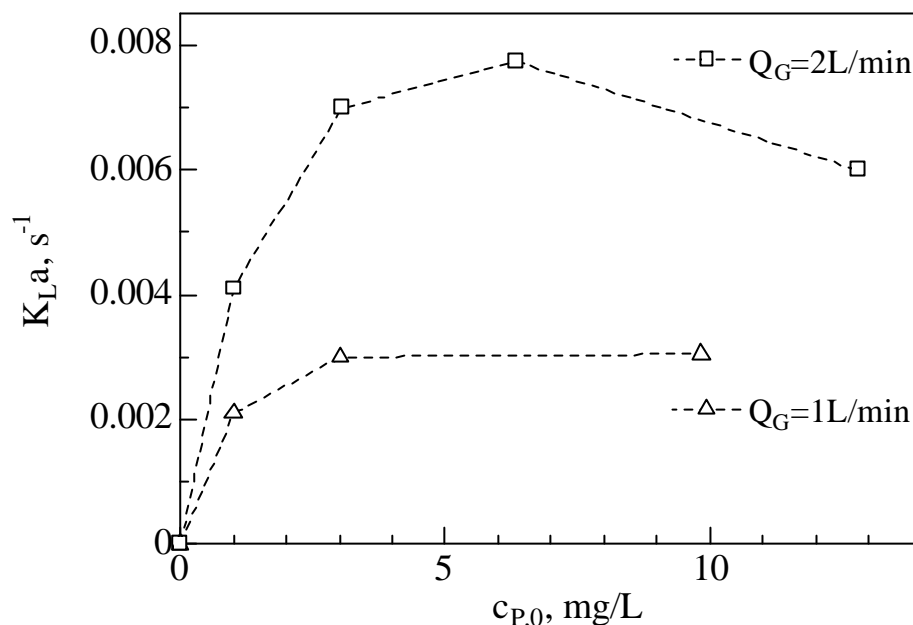

Figure 4.4. The increase of the mass transfer coefficient as a function of the initial PCE bulk liquid concentration.

The increase of the mass transfer coefficient depends on the bulk liquid concentration and on the applied gas flow rate (Fig. 4.4). It can be accounted for by an empirical factor α, expressed as a ratio of the mass transfer coefficient where the effect of PCE is significant to the mass transfer coefficient where the effect of the increased PCE concentration is still negligible. It appears that water-PCE solutions and pure water exhibit rather different behaviors arising from the differences in the bubble formation process due to sparger type and coalescence phenomena. Predictions of mass transfer based on the popular Eq. (4-14) might lead to large errors in predicting the mass transfer coefficient, once the concentration of PCE in the bulk liquid becomes large enough to cause a change in the physical characteristics of the bulk.
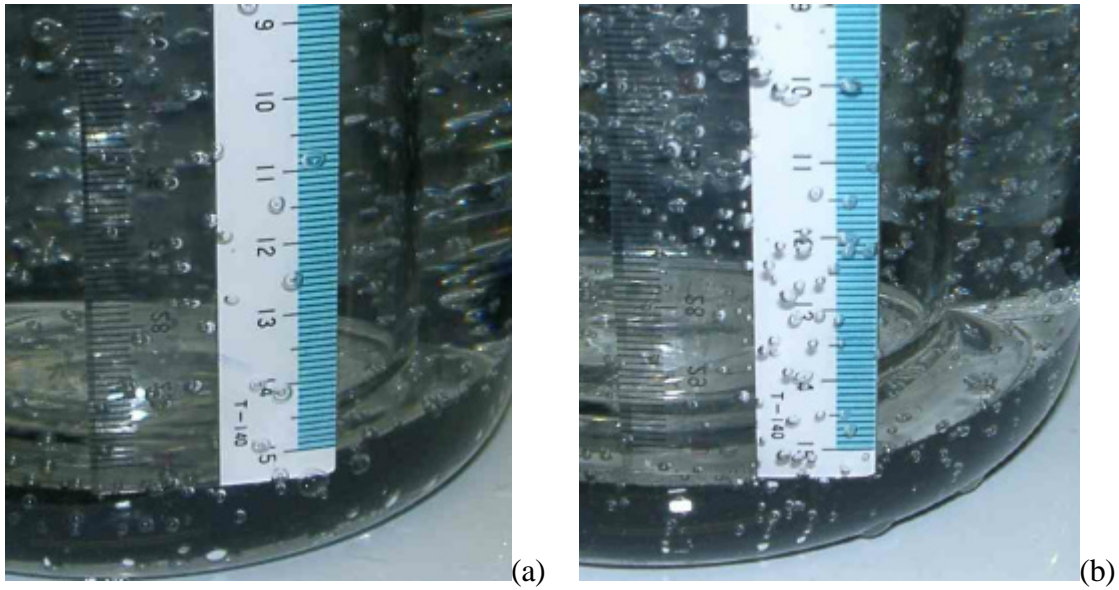
(a)   (b)

Figure 4.5. Effect of PCE on bubble size. (a) Deionized water. (b) Deionized water and PCE. $Q_G = 1L/min$.

Figure 4.5 shows comparative photographs of bubbles in deionized water and water – PCE solutions under the same operating conditions. In Fig. 4.5(b) the water was spiked with the PCE solution and PCE gas was bubbled through the gas distributor. It can be observed that bubbles formed at the gas distributor are substantially smaller in the presence of PCE, compared to the bubbles formed in pure water. It can be concluded that the role of gas distributor is important parameter and will have to be accounted for in the optimization procedure.

The bubble diameter was not measured in this study, but can be predicted from the correlations as an approximation. As stated earlier in the work of Öztürk *et al*. (1987), the volume-surface mean diameter (d_{vs}) can be assumed almost constant with a value of cca 3 mm. For the approximation, bubble diameter was also calculated using two correlations:

(a) the equation proposed by Calderbank (1967), which was developed on the basis of Kolmogoroff's isotropic turbulence theory:

$$d_{vs} = C_1 \cdot \frac{\sigma_L^{0.6}}{\left(\dfrac{P_t}{V_L}\right)^{0.4} \cdot \rho_L^{0.2}} \cdot \varepsilon_G^n \cdot \left(\frac{\eta_G}{\eta_L}\right)^{0.25} + C_2 \qquad (4\text{-}26)$$

where C_1, C_2 and n are empirical constants which depend on the aqueous medium, and are equal to 4.15, 0.0009 and 0.5 for pure liquids, respectively.

(b)The empirical correlation proposed by Gaddis for a porous plate sparger

$$d_{vs} = 2.15 \cdot 10^{-3} \left(\frac{P_t}{V_L}\right)^{0.16} \qquad (4\text{-}27)$$

The energy dissipation rate P_t/V_L for bubble columns with effective gas spargers can be given as

$$\frac{P_t}{V_L} = u_G \rho_L (1 - \varepsilon_G) g \qquad (4\text{-}28)$$

Table 4.1. Mass transfer characteristics of the UV-BCR as a function of superficial gas velocity, u_G. d_{vs} and P_t/V_L were calculated by Eqs. (4-27) and (4-28) respectively.

u_G,	ε_G,	P_t/V_L,	d_{vs},[a]	d_{vs},[b]	$a = 6\varepsilon_G/d_{vs}$,[a]	K_La,	k_L,
m/s	/	W/m^3	m	m	1/m	1/s	m/s
0	0	0	0	0	0	0	0
0.002	0.00945	19,5	0.00325	0.00345	17.4	0.0021	0.000114
0.003	0.01439	29.2	0.00337	0.00369	25.6	0.0031	0.00012
0.004	0.0183	38.7	0.00339	0.00385	32.4	0.0040	0.00012
0.006	0.0284	57.5	0.00354	0.0041	48.0	0.0059	0.000123

Both correlations predict the size of the bubbles at cca 3 mm; however, the correlation from

Gaddis predicts quite a high influence of the energy dissipation rate on bubble size, which seems to be an overestimation, when compared to the size evaluated with the pictures. It should be noted that pictures show only approximate size of the bubbles, as the equipment (digital camera) was not appropriate for precise evaluation of the size by photographic technique.

The true mass transfer coefficient is difficult to measure. The order of magnitude of this parameter is between 10^{-4} and 10^{-5} m/s. It can also be estimated based on the mass transfer theories or by dividing the experimentally obtained $k_L a$ values by the specific surface area. The values of k_L presented in Table 4.1 were obtained by the latter technique and are in good agreement with the values calculated from the relation based in the Higbie penetration theory. This theory assumes that the effective contact time in bubble columns is given by ratio d_{sv}/u_s:

$$k_L = 1.13 \sqrt{\frac{D_{PCE} u_G}{d_{vs} \varepsilon_G}} \tag{4-29}$$

Based on the two-film theory by Lewis and Whitman (1924) Munz and Roberts (1989) proposed a way to calculate the relative resistance to either gas or liquid side mass transfer by introducing the proportionality factor Ψ. The proportionality factor is defined with oxygen as the reference compound and can be therefore related to any other volatile compound, given that their diffusivity and Henry's constant are known. Exponent "n" in Eq. (4-30) varies between $0.5 \leq n \leq 1$, depending on the theory from which the ratio of diffusivities is used, but it was found that values of 0.5 and 0.66 usually apply for liquid phase controlled as well as gas phase controlled mass transfer.

$$\Psi = \frac{K_{L,i} a}{K_{L,O_2} a} = \left[\frac{D_{L,i}}{D_{L,O_2}} \right]^n \left[\frac{R_L / R_G}{1 + R_L / R_{GO_2}} \right] = \left[\frac{D_{L,i}}{D_{L,O_2}} \right]^n \left[1 + \frac{1}{(k_G / k_L) m_i} \right]^{-1} \tag{4-30}$$

The Ψ value of PCE for specific power inputs P_t/V_L, ranging from 0.84 to 320 W/m^3 was reported to be 0.61. In this case, using n=0.5, k_G/k_L was found to be 75, meaning that mass transfer is controlled by transfer through the liquid film, and that the overall mass transfer coefficient K_La can be written as k_La and only liquid side film resistance during mass transfer needs to be considered.

4.5 CONCLUSIONS

From the analysis of the mass transfer performance it can be concluded that with application of low superficial gas velocities, the UV-BCR operated in the homogeneous bubbly flow regime and the volumetric mass transfer coefficient was proportional to the superficial gas velocity. The bubble rise velocity was cca 22 cm/s. The mass transfer coefficient could be predicted based on the proposed empirical correlation when operating with low bulk PCE concentrations. As a special observation the mass transfer increased with increasing bulk liquid concentration, indicating that the effect of the gas distributor on the mass transfer performance must be known. The distributor effect will depend on the type of molecule, its concentration, gas flow rate and the design of the sparging device, making it an important design and optimization parameter.

When the sequence-making internal component was in the reactor, the hydrodynamic behavior of the reactor changed, and could be approximated by equations valid for the transition, churn-turbulent regime.